JOC Article

Molecular Encapsulation via Metal-to-Ligand Coordination in a Cu(I)-Folded Molecular Basket

Stephen Rieth, Zhiqing Yan, Shijing Xia, Matthew Gardlik, Albert Chow, Gideon Fraenkel, Christopher M. Hadad, and Jovica D. Badjić*

Department of Chemistry, The Ohio State University, 100 W. 18th Avenue, Columbus, Ohio 43210

badjic@chemistry.ohio-state.edu

Received April 5, 2008

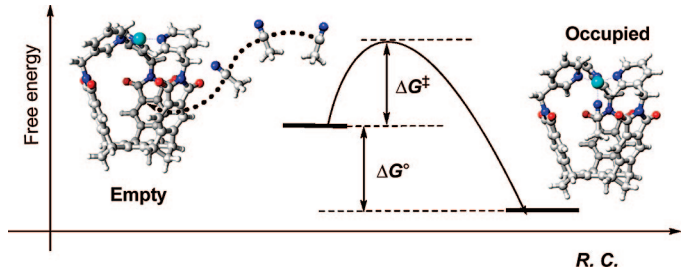

A molecular basket, composed of a semirigid C_{3v} symmetric *tris*-norbornadiene framework and three pyridine flaps at the rim, has been shown to coordinate to a Cu(I) cation and thereby fold in a multivalent fashion. The assembly was effective ($K_a = 1.73 \pm 0.08 \times 10^5$ M^{-1}) and driven by enthalpy ($\Delta H° = -7.2 \pm 0.1$ kcal/mol, $\Delta S° = -0.25$ eu). Variable temperature ^{1}H NMR studies, assisted with 2D COSY and ROESY investigations, revealed the existence of Cu(I)-folded basket $\mathbf{10_b}$ with a molecule of acetonitrile occupying its interior and coordinated to the metal. Interestingly, $\mathbf{10_b}$ is in equilibrium with Cu(I)-folded $\mathbf{10_a}$, whose inner space is solvated by acetone or chloroform. The incorporation of a molecule of acetonitrile inside $\mathbf{10_a}$ was found to be driven by enthalpy ($\Delta H° = -3.3 \pm 0.1$ kcal/mol), with an apparent loss in entropy ($\Delta S° = -9.4 \pm 0.4$ eu); this is congruent with a complete immobilization of acetonitrile and release of a "loosely" encapsulated solvent molecule during $\mathbf{10_{a/b}}$ interconversion. From an Eyring plot, the activation enthalpy for incorporating acetonitrile into $\mathbf{10_a}$ was found to be positive ($\Delta H^‡ = 6.5 \pm 0.5$ kcal/mol), while the activation entropy was negative ($\Delta S^‡ = -20 \pm 2$ eu). The results are in agreement with an exchange mechanism whereby acetonitrile "slips" into an "empty" basket through its side aperture. In fact, DFT (BP86) calculations are in favor of such a mechanistic scenario; the calculations suggest that opening of the basket's rim to exchange guests is energetically demanding and therefore less feasible.

Introduction

The modulation of chemical reactivity in biological systems develops via a subtle interplay of molecular recognition, dynamics, and trafficking in line with a synchronized formation and rupture of covalent bonds.[1] Understanding the complexity of biological molecules capable of promoting chemical transformations and facilitating their mechanism of action presents a great challenge and, at the same time, is a source of inspiration for both experimentalists and theoreticians. In that vein, major advances in the field of chemical catalysis necessitate the incorporation of dynamic elements of design[2] into artificial systems to resemble molecular machines.[3] Yet, a steady development of complex molecular assemblies[4] and elucidation of their operation[5] merit a profound consideration for expanding fundamental understanding of the relationship between synchronized molecular motion, encapsulation, dynamics, and reactivity in artificial environments.[6]

Molecular containers,[7] such as carcerands, calixarenes, self-assembled capsules, and metal-assembled cages, were originally designed to trap a target compound, and in a way these hosts belong to a family of biomimetic compounds.[8] Housing a guest,

(1) (a) McCammon, J. A.; Northrup, S. H. *Nature* **1981**, *293*, 316–317. (b) Wlodek, S. T.; Clark, T. W.; Scott, L. R.; McCammon, J. A. *J. Am. Chem. Soc.* **1997**, *119*, 9513–9522. (c) Benkovic, S. J.; Hammes-Schiffer, S. *Science* **2003**, *301*, 1196–1202. (d) Gunasekaran, K.; Buyong, M.; Nussinov, R. *Proteins* **2004**, *53*, 433–443. (e) Williams, D. H.; Stephens, E.; O'Brien, D. P.; Zhou, M. *Angew. Chem., Int. Ed.* **2004**, *43*, 6596–6616. (f) Zhang, X.; Houk, K. N. *Acc. Chem. Res.* **2005**, *38*, 379–385. (g) Engelkamp, Hans, H.; Nikos, S.; Hofkens, J.; De Schryver, F. C.; Nolte, R. J. M.; Rowan, A. E. *Chem. Commun.* **2006**, *9*, 935–940. (h) Zhang, X.; DeChancie, J.; Gunaydin, H.; Chowdry, A. B.; Clemente, F. R.; Smith, A. J. T.; Handel, T. M.; Houk, K. N. *J. Org. Chem.* **2008**, *73*, 889–899.

10.1021/jo800748k CCC: $40.75
Published on Web 06/04/2008

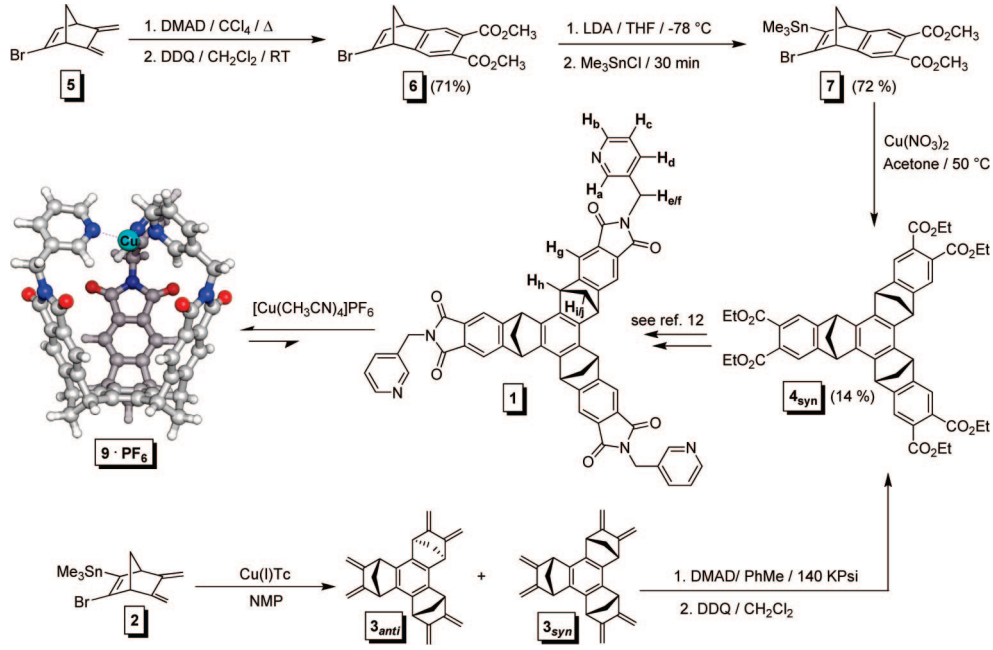

FIGURE 1. Synthetic routes for the preparation of molecular basket **1** via the earlier developed[12] (bottom) and new method (top). ^{1}H NMR spectroscopic assignment of **1** and chemical structure of folded [**9** × PF_6].

inside a container, permitted its increased kinetic and thermodynamic stability[9] and also provided a molecular reaction domain.[10] In recent times, however, there has been a growing interest for elucidating the dynamic behavior of such assemblies, and in particular for scrutinizing the mechanism of guest exchange and its relation to chemical reactivity.[2,5]

In view of such activities, this study reports on the design and preparation of a copper(I)-folded molecular basket[11] with intriguing conformational behavior and operational mechanism for guest incorporation that could allow for manipulating the kinetic stability and position of the guest. The basket belongs to a family of hosts,[12] comprising a semirigid C_{3v} symmetrical *tris*-norbornadiene framework that gives rise to its concave shape (Figure 1). Three aromatic rings, incorporating transition metal chelating sites, are installed at the rim to act as dynamic appendages in controlling the folding and thus forming the basket's "dynamic" interior. As a result, the location and the in/out trafficking of the guest(s) has been speculated to be controlled by a combination of constrictive binding and metal-to-ligand coordination. Indeed, the experimental and theoretical studies of these Cu(I)-folded molecular baskets revealed, for the first time, an operational mechanism where metal-to-ligand coordination in combination with the basket's folding behavior dominates the in/out exchange of an encapsulated guest. The assembly exemplifies a crude mimic of a nitrogen-containing metalloenzyme active site that unifies the concepts of molecular confinement and metal-to-ligand directed encapsulation in a dynamic space. This study demonstrates the utility of devising ways for controlling molecular trafficking, and perhaps reactivity, in programmed chemical environments where the reaction effectiveness is manageable to a greater extent.

Results and Discussion

Synthesis. Our originally developed procedure for the preparation of **1**[12] has been considerably improved (Figure 1). A transition metal catalyzed *tris*-annulation of racemic norbornene **2** was reported to give diastereomer $\mathbf{3}_{anti}$ in excess.[12a] Scarce amounts of the desired *syn* isomer were obtained, necessitating a lengthy procedure for separating the two stereoisomeric compounds. Furthermore, cycloaddition of the reactive dienophile, dimethyl acetylenedicarboxylate (DMAD), to $\mathbf{3}_{syn}$ required high pressure (140 KPsi) and long reaction times for completion, which severely limited our capacity to run the reaction on a

(2) Davis, A. V.; Yeh, R. M.; Raymond, K. N. *Proc. Natl. Acad. Sci. U.S.A.* **2002**, *99*, 4793–4796.

(3) (a) Ismagilov, R. F.; Schwartz, A.; Bowden, N.; Whitesides, G. M. *Angew. Chem., Int. Ed.* **2002**, *41*, 652–654. (b) Badjic, J. D.; Balzani, V.; Credi, A.; Silvi, S.; Stoddart, J. F. *Science* **2004**, *303*, 1845–1849. (c) Hernandez, J. V.; Kay, E. R.; Leigh, D. A. *Science* **2004**, *306*, 1532–1537. (d) Eelkema, R.; Pollard, M. M.; Vicario, J.; Katsonis, N.; Ramon, B. S.; Bastiaansen, C. W. M.; Broer, D. J.; Feringa, B. L. *Nature* **2006**, *440*, 163.

(4) Philp, D.; Stoddart, J. F. *Angew. Chem., Int. Ed. Engl.* **1996**, *35*, 1155–1196. (b) Whitesides, G. M.; Grzybowski, B. *Science* **2002**, *295*, 2418–2421. (c) Reinhoudt, D. N.; Crego-Calama, M. *Science* **2002**, *295*, 2403–2407. (d) Fialkowski, M.; Bishop, K. J. M.; Klajn, R.; Smoukov, S. K.; Campbell, C. J.; Grzybowski, B. A *J. Phys. Chem. B* **2006**, *110*, 2482–2496.

(5) (a) Palmer, L. C.; Rebek, J., Jr. *Org. Biomol. Chem.* **2004**, *2*, 3051–3059. (b) Turner, D. R.; Pastor, A.; Alajarin, M.; Steed, J. W. *Struct. Bonding (Berlin)* **2004**, *108*, 97–168. (c) Purse, B. W.; Rebek, J., Jr. *Proc. Natl. Acad. Sci. U.S.A.* **2005**, *102*, 10777–10782. (d) Sauvage, J.-P. *Chem. Comm.* **2005**, *12*, 1507–1510. (e) Karlen, S. D.; Garcia-Garibay, M. A. *Top. Curr. Chem.* **2005**, *262*, 179–227. (f) Pluth, M. D.; Raymond, K. N. *Chem. Soc. Rev.* **2007**, *36*, 161–171.

(6) (a) Feiters, M. C.; Gebbink, R. J. M.; Klein; Schenning, A. P. H. J.; van Strijdonck, G. P. F.; Martens, C. F.; Nolte, R. J. M. *Pure Appl. Chem.* **1996**, *68*, 2163–2170. (b) Breslow, R.; Dong, S. D. *Chem. Rev* **1998**, *98*, 1997–2011. (c) Yoshizawa, M.; Kusukawa, T.; Fujita, M.; Yamaguchi, K. *J. Am. Chem. Soc.* **2000**, *122*, 6311–6312. (d) Merlau, M. L.; Del Pilar, M. M.; Nguyen, S. T.; Hupp, J. T. *Angew. Chem., Int. Ed.* **2001**, *40*, 4239–4242. (e) Thordarson, P.; Nolte, R. J. M.; Rowan, A. E. *Aust. J. Chem.* **2004**, *57*, 323–327. (f) Yan, Z.; Chang, Y.; Mayo, D.; Maslak, V.; Xia, S.; Badjić, J. D. *Org. Lett.* **2006**, *8*, 3697–3700. (g) Nishioka, Y.; Yamaguchi, T.; Yoshizawa, M.; Fujita, M. *J. Am. Chem. Soc.* **2007**, *129*, 7000–7001. (h) Pluth, M. D.; Bergman, R. G.; Raymond, K. N. *Angew. Chem., Int. Ed.* **2007**, *46*, 8587–8589. (i) Hooley, R. J.; Restorp, P.; Iwasawa, T.; Rebek, J., Jr. *J. Am. Chem. Soc.* **2007**, *129*, 15639–15643. (j) Yoon, H. J.; Heo, J.; Mirkin, C. A. *J. Am. Chem. Soc.* **2007**, *129*, 14182–14183. (k) Natarajan, A.; Kaanumalle, L. S.; Jockusch, S.; Gibb, C. L. D.; Gibb, B. C.; Turro, N. J.; Ramamurthy, V. *J. Am. Chem. Soc.* **2007**, *129*, 4132–4133. (l) Gottschalk, T.; Jaun, B.; Diederich, F. *Angew. Chem., Int. Ed.* **2007**, *46*, 260–264.

larger scale and within a reasonable time frame. The newly developed procedure (Figure 1) has been optimized to address these difficulties and should facilitate future studies of molecular baskets.

The cycloaddition of DMAD to **5**, in boiling CCl_4, yielded **6**, after a DDQ aromatization step. Compound **6** was then stannylated to give **7**, in an optimized protocol that required a rapid quenching of the vinyl-carbanion with trimethyltin chloride. The cyclotrimerization of **7** into $\mathbf{4}_{syn}$ was attempted following a number of routes, originally developed by De Lucchi et al.[13] In particular, we found that the $Cu(NO_3)_2 \cdot (H_2O)_{2.5}$ salt[14] promoted the transformation in acetone (24% yield), with a satisfactory diastereoselectivity (*syn*/*anti* = 1:1.4). Intriguingly, when this reaction is compared to the cyclotrimerization in THF (2% yield), the templating role[12c,15] of acetone in the formation of $\mathbf{4}_{syn}$ can be envisioned; this solvent is, in particular, known to effectively fill the cavity of $\mathbf{4}_{syn}$ in the solid state.[12b] The mechanistic details for the cyclotrimerizations promoted with Cu(II) have, in fact, been addressed.[14d] A chain-type cyclization pathway has been discounted in the advantage of the initial Sn−Sn type coupling of the racemic halostannanes (in this case, **7**). The observed enantiodiscrimination in the formation of $\mathbf{4}_{syn}$ is consistent with such a mechanistic scenario. The initial Sn−Sn heterocouplings could be kinetically promoted, in the presence of the templating solvent molecules, and over the competing homocouplings to give rise to the *syn* product. Hexaester $\mathbf{4}_{syn}$ was easily separated from $\mathbf{4}_{anti}$ by column chromatography and subsequently converted to the desired **1**, in accord with the already published procedure.[12]

^{1}H NMR Spectroscopic Titration. An incremental addition of $[Cu(I)(CH_3CN)_4]PF_6$ to a solution of **1** ($CD_3COCD_3/CDCl_3$ = 5:3) prompted considerable changes in its ^{1}H NMR spectrum (Figure 2A). The signal for the $\mathbf{H}_a$ proton shifted upfield ($\Delta\delta_{max}$ = 0.6 ppm), while the resonances corresponding to the $\mathbf{H}_{c/d}$ signals moved downfield ($\Delta\delta_{max}$ = 0.3 and 0.5 ppm, respectively). Interestingly, the $\mathbf{H}_b$ resonance was only slightly perturbed with increasing amounts of Cu(I). All of the spectroscopic changes were persistent until an equimolar (1:1) ratio of Cu(I):**1** was reached, and no considerable ^{1}H NMR shifts were detected when an "excess" of the transition metal was present (Figure 2B). The observed ^{1}H NMR changes are thus akin to those evidenced in the addition of Ag(OTf) to **1**,[12b] suggesting a comparable mode of metal-to-ligand coordination. However, this time, a small and soft Cu(I) cation mediated the formation of C_3 symmetrical and folded basket [**9** × PF_6] (Figure 1), and on average, there is a rapid interconversion between **1** and Cu(I):**1** (i.e., [**9** × PF_6]) on the NMR time scale (Figure 2A). On the basis of the ^{1}H NMR titration, the formation of [**9** × PF_6] was indeed effective: the break in the titration curve at the 1:1 host/guest ratio[16] is quite obvious (Figure 2B). A nonlinear least-squares analysis of the titration data, furthermore, suggested that the association constant is greater than 10^5 M^{-1} (Figure 2B).

Interestingly, the ^{1}H NMR line shapes of the resonances for **1** appeared considerably broadened before an equimolar amount of the transition metal was added to the solution (Figure 2A). The signals, however, sharpened at and after the equimolar point. An exchange process between **1** and [**9** × PF_6], was presumably occurring at an intermediate rate. Indeed, a variable temperature ^{1}H NMR study of **1**, containing 0.5 mol equiv. of $[Cu(I)(CH_3CN)_4]PF_6$, revealed decoalescence of the signals at 240 K.[18] Two sets of resonances appeared: one corresponding to the Cu(I) assembled basket and another one to free **1** in a fast equilibrium with its coordinated form.[18]

Spherically symmetrical and diamagnetic Cu(I) of the electron configuration d^{10} is known to readily oxidize into paramagnetic

(7) (a) Cram, D. J.; Cram, J. M. In *Container Molecules and Their Guests*; Stoddart, J. F., Series Ed.; The Royal Society of Chemistry: Cambridge, U.K., 1994. (b) Rebek, J., Jr. *Pure Appl. Chem.* **1996**, *68*, 1261–1266. (c) Jacopozzi, P.; Dalcanale, E. *Angew. Chem., Int. Ed. Engl.* **1997**, *36*, 613–615. (d) De Mendoza, J. *Chem. Eur. J.* **1998**, *4*, 1373–1377. (e) Jasat, A.; Sherman, J. C. *Chem. Rev.* **1999**, *99*, 931–967. (f) Rudkevich, D. M.; Rebek, J., Jr. *Eur. J. Org. Chem.* **1999**, *9*, 1991–2005. (g) MacGillivray, L. R.; Holman, K. T.; Atwood, J. L. *J. Supramol. Chem.* **2002**, *1*, 125–130. (h) Caulder, D. L.; Brueckner, C.; Powers, R. E.; Koenig, S.; Parac, T. N.; Leary, J. A.; Raymond, K. N. *J. Am. Chem. Soc.* **2001**, *123*, 8923–8938. (i) Corbellini, F.; Knegtel, R. M. A.; Grootenhuis, P. D. J.; Crego-Calama, M.; Reinhoudt, D. N. *Chem. Eur. J.* **2005**, *11*, 298–307. (j) Lagona, J.; Mukhopadhyay, P.; Chakrabarti, S.; Isaacs, L. *Angew. Chem., Int. Ed.* **2005**, *44*, 4844–4870. (k) Fox, O. D.; Cookson, J.; Wilkinson, E. J. S.; Drew, M. G. B.; MacLean, E. J.; Teat, S. J.; Beer, P. D. *J. Am. Chem. Soc.* **2006**, *128*, 6990–7002. (l) Yamanaka, M.; Yamada, Y.; Sei, Y.; Yamaguchi, K.; Kobayashi, K. *J. Am. Chem. Soc.* **2006**, *128*, 1531–1539.

(8) Breslow, R. *Chem. Biol.* **1998**, *5*, R27–R28.

(9) (a) Warmuth, R. *Eur. J. Org. Chem.* **2001**, *3*, 423–437. (b) Rebek, J., Jr. *Nature* **2006**, *444*, 557.

(10) (a) Breslow, R. *Acc. Chem. Res.* **1995**, *28*, 146–153. (b) Warmuth, R. *J. Inclusion Phenom. Mol. Recognit. Chem.* **2000**, *37*, 1–38. (c) Vriezema, D. M.; Aragones, M. C.; Elemans, J. A. A. W.; Cornelissen, J. J. L. M.; Rowan, A. E.; Nolte, R. J. M. *Chem. Rev.* **2005**, *105*, 1445–1489. (d) Yoshizawa, M.; Tamura, M.; Fujita, M. *Science* **2006**, *312*, 251–254. (e) Kuil, M.; Soltner, T.; Van Leeuwen, P. W. N. M.; Reek, J. N. H. *J. Am. Chem. Soc.* **2006**, *128*, 11344–11345. (f) Leung, D. H.; Bergman, R. G.; Raymond, K. N. *J. Am. Chem. Soc.* **2007**, *129*, 2746–2747. (g) Zecchina, A.; Groppo, E.; Bordiga, S. *Chem. Eur. J.* **2007**, *13*, 2440–2460.

(11) For selected examples of metallocavitands, see: (a) Kuroda, Y.; Hiroshige, T.; Sera, T.; Shiroiwa, Y.; Tanaka, H.; Ogoshi, H. *J. Am. Chem. Soc.* **1989**, *111*, 1912–1913. (b) Rudkevich, D. M.; Huck, W. T. S.; van Veggel, F. C.J. M.; Reinhoudt, D. N. In *Transition Metals in Supramolecular Chemistry*; Fabbrizzi, L., Poggi, A., Eds.; Kluwer Academic Publishers: Dodrecht,1994; pp 329−349. (c) Xu, W.; Vittal, J. J.; Puddephatt, R. J. *J. Am. Chem. Soc.* **1995**, *117*, 8362–71. (d) Bonar-Law, R. P.; Sanders, J. K. M. *J. Chem. Soc., Perkin Trans. 1* **1995**, *3085*, 96. (e) Wieser-Jeunesse, C.; Matt, D.; De Cian, A. *Angew. Chem., Int. Ed.* **1998**, *37*, 2861–2864. (f) Fan, M.; Zhang, H.; Lattman, M. *Chem. Commun.* **1998**, *1*, 99–100. (g) Seneque, O.; Rager, M.-N.; Giorgi, M.; Reinaud, O. *J. Am. Chem. Soc.* **2000**, *122*, 6183–6189. (h) Luecking, U.; Chen, J.; Rudkevich, D. M.; Rebek, J., Jr. *J. Am. Chem. Soc.* **2001**, *123*, 9929–9934. (i) Starnes, S. D.; Rudkevich, D. M.; Rebek, J., Jr. *J. Am. Chem. Soc.* **2001**, *123*, 4659–69. (j) Rondelez, Y.; Bertho, G.; Reinaud, O. *Angew. Chem., Int. Ed.* **2002**, *41*, 1044–1046. (k) Rondelez, Y,; Rager, M.-N.; Duprat, A.; Reinaud, O. *J. Am. Chem. Soc.* **2002**, *124*, 1334–1340. (l) Seneque, O.; Rager, M-N.; Giorgi, M.; Prange, T.; Tomas, A.; Reinaud, O. *J. Am. Chem. Soc.* **2005**, *127*, 14833–14840. (m) Colasson, B.; Save, M.; Milko, P.; Roithova, J.; Schroeder, D.; Reinaud, O. *Org. Lett.* **2007**, *9*, 4987–4990.

(12) (a) Maslak, V.; Yan, Z.; Xia, S.; Gallucci, J.; Hadad, C. M.; Badjić, J. D. *J. Am. Chem. Soc.* **2006**, *128*, 5887–5894. (b) Yan, Z.; Xia, S.; Gardlik, M.; Seo, W.; Maslak, V.; Gallucci, J.; Hadad, C. M.; Badjić, J. D. *Org. Lett.* **2007**, *9*, 2301–2304. (c) Yan, Z.; McCracken, T.; Xia, S.; Maslak, V.; Gallucci, J.; Hadad, C. M.; Badjić, J. D. *J. Org. Chem.* **2008**, *73*, 355–363.

(13) (a) Fabris, F.; De Martin, A.; De Lucchi, O. *Tetrahedron Lett.* **1999**, *40*, 9121–9124. (b) Paulon, A.; Cossu, S.; De Lucchi, O.; Zonta, C. *Chem. Commun.* **2000**, *19*, 1837–1838. (c) Cossu, S.; Cimenti, C.; Peluso, P.; Paulon, A.; De Lucchi, O. *Angew. Chem., Int. Ed.* **2001**, *40*, 4086–4089. (d) Cossu, S.; De Lucchi, O.; Paulon, A.; Peluso, P.; Zonta, C. *Tetrahedron Lett.* **2001**, *42*, 3515–3518. (e) Borsato, G.; De Lucchi, O.; Fabris, F.; Groppo, L.; Lucchini, V.; Zambon, A. *J. Org. Chem.* **2002**, *67*, 7894–7897. (f) Borsato, G.; De Lucchi, O.; Fabris, F.; Lucchini, V.; Pasqualotti, M.; Zambon, A. *Tetrahedron Lett.* **2002**, *44*, 561–563. (g) Fabris, F.; Bellotto, L.; De Lucchi, O. *Tetrahedron Lett.* **2003**, *44*, 1211–1213. (h) Zonta, C.; Fabris, F.; De Lucchi, O. *Org. Lett.* **2005**, *7*, 1003–1006.

(14) (a) Ghosal, S.; Luke, George, P.; Kyler, K. S. *J. Org. Chem.* **1987**, *52*, 4296–4298. (b) Beddoes, R. L.; Cheeseright, T.; Wang, J.; Quayle, P. *Tetrahedron Lett.* **1995**, *36*, 283–286. (c) Durr, R.; Cossu, S.; Lucchini, V.; De Lucchi, O. *Angew. Chem., Int. Ed.* **1997**, *36*, 2805–2807. (d) Zonta, C.; Cossu, S.; Peluso, P.; De Lucchi, O. *Tetrahedron Lett.* **1999**, *40*, 8185–8188. (e) Peluso, P.; De Lucchi, O.; Cossu, S. *Eur. J. Org. Chem.* **2002**, *23*, 4032–4036.

(15) For the principles of template-directed synthesis, see:(a) Sherman, J. *Chem. Commun.* **2003**, *14*, 1617–1623. (b) Arico, F.; Badjić, J. D.; Cantrill, S. J.; Flood, A. H.; Leung, K. C. F.; Liu, Y.; Stoddart, J. F. *Top. Curr. Chem.* **2005**, *249*, 203–259. (c) Gibb, C. L. D.; Gibb, B. C. *Chem. Commun.* **2007**, *16*, 1635–1637.

(16) Wilcox, C. *Frontiers in Supramolecular Organic Chemistry and Photochemistry*; Schneider, H.-J., Durr, H., Eds.; Wiley-VCH: Weinheim, 1991; pp 123−143.

(17) Connors, K. A. *Binding Constants, The Measurement of Molecular Complex Stability*; Wiley-Interscience: New York, 1987; pp 24−28.

(18) See Supporting Information for more details.

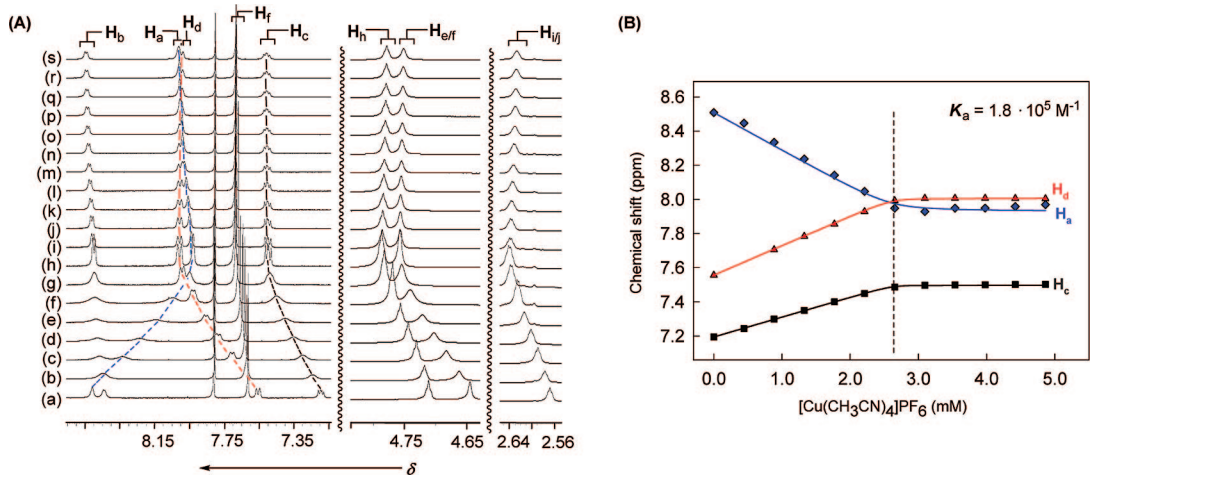

FIGURE 2. (A) A series of ^{1}H NMR spectra (400 MHz, 300 K; $CD_3COCD_3/CDCl_3$ = 5:3) of **1** (2.60 mM), recorded after a gradual addition of 53.0 mM of standard solution of $[Cu(I)(CH_3CN)_4]PF_6$, such that the final mixture comprises (a) 0, (b) 0.17, (c) 0.34, (d) 0.51, (e) 0.68, (f) 0.85, (g) 1.02, (h) 1.19, (i) 1.36, (j) 1.53, (k) 1.70, (l) 1.87, (m) 2.04, (n) 2.21, (o) 2.38, (p) 2.55, (q) 2.72, (r) 2.89, and (s) 3.06 molar equiv of Cu(I). (B) The nonlinear curve fitting of the ^{1}H NMR chemical shifts of the $\mathbf{H_a/H_c/H_d}$ resonances to a 1:1 equilibrium model.[16,17]

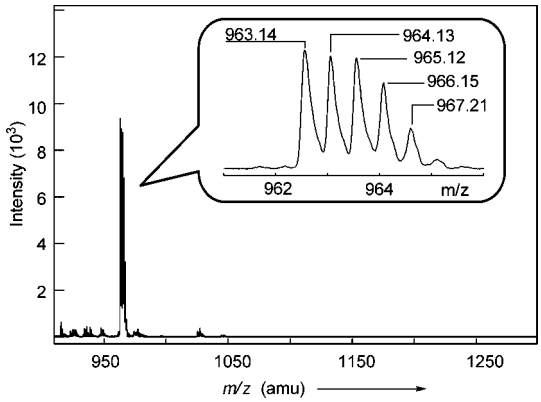

FIGURE 3. Low-resolution MALDI (TOF) mass spectrum of an equimolar mixture of **1** and $[Cu(I)(CH_3CN)_4]PF_6$ (2.60 mM), with a major signal at m/z = 963.14 amu, corresponding to the $[\mathbf{1}{:}Cu]^+$ cation. In the inset, the isotopic distribution is shown.

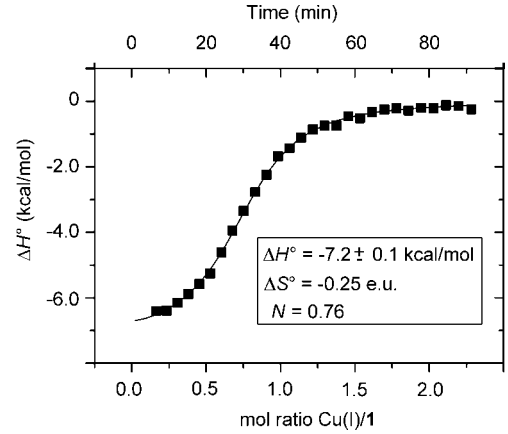

FIGURE 4. Isothermal titration calorimetry data for the gradual addition of a 1.00 mM standard solution of $[Cu(I)(CH_3CN)_4]PF_6$ to a 0.10 mM solution of **1** (CH_3CN), under an atmosphere of nitrogen. Computer simulated curve fitting (below) afforded the thermodynamic parameters for the assembly of $[\mathbf{9} \times PF_6]$.

Cu(II) that, in turn, causes broadening of ^{1}H NMR signals.[19] For that reason, our titration experiments were conducted under a nitrogen atmosphere, as traces of oxygen were noted to cause the rapid oxidation of the chelated metal and the loss of ^{1}H NMR signals.

Mass Spectrometric Analysis. Matrix-assisted laser desorption/ionization (MALDI) mass spectrometry comprises a soft ionization method for generating ions, thereby allowing a nondestructive vaporization and ionization of large molecular weight compounds.[20] The characterization of fragile noncovalent assemblies has, in particular, been proven feasible with the method,[21] and we conducted MALDI-TOF (time-of-flight) experiments to ascertain the nature of our Cu(I)-mediated assembly(ies) (Figure 3). On the basis of the exclusive appearance of a peak at 963.14 amu (Figure 3), corresponding to the $[\mathbf{1}{:}Cu]^+$ cation, the affinity of Cu(I) toward polydentate **1** was verified to be high. The observed signal, despite suggesting a 1:1 stoichiometry of the metal coordinated to the basket, reveals the absence of any apical ligand(s) or an encapsulated molecule in the cavity of $[\mathbf{1}{:}Cu]^+$. The assembly in the gas phase, evidently, incorporates a trigonal Cu(I) with no preference for coordinating a labile monodentate acetonitrile. Moreover, adding a better σ electron donor, such as imidazole, to the assembly, did not reveal any new signals in MALDI,[18] yet again confirming the identity and stability of the gas-phase dominating $[\mathbf{1}{:}Cu]^+$ cation.

Isothermal Titration Calorimetry (ITC). The thermodynamic profile for the formation of $[\mathbf{9} \times PF_6]$ (Figure 1) was further examined with isothermal titration calorimetry (ITC, Figure 4).

A stock solution of $[Cu(CH_3CN)_4]PF_6$ (1.00 mM, CH_3CN) was added in portions to a solution of **1** (0.10 mM, CH_3CN) contained in the sample cell. The required anaerobic atmosphere, for preventing highly exothermic Cu(I) oxidation, was secured by completing the experiment in an Atmos-Bag filled with nitrogen at a positive pressure. The heat released in the assembly ($\Delta H° = -7.2 \pm 0.1$ kcal/mol) gave the binding isotherm (Figure 4), which upon fitting to a one-site model revealed $K_a = (1.73 \pm 0.08) \times 10^5$ M^{-1} ($\Delta G° = -7.2$ kcal/mol, 300 K) and N =

(19) (a) Smith, D. R. *Coord. Chem. Rev.* **1998**, *172*, 457–573. (b) van der, V. J. I.; Meyer, F. *Top. Organomet. Chem.* **2007**, *22*, 191–240.
(20) Zenobi, R.; Breuker, K.; Knochenmuss, R.; Lehmann, E.; Stevenson, E. *Adv. Mass Spectrom.* **2001**, *15*, 143–149.
(21) (a) Jolliffe, K. A.; Calama, M. C.; Fokkens, R.; Nibbering, N. M. M.; Timmerman, P.; Reinhoudt, D. N. *Angew. Chem., Int. Ed.* **1998**, *37*, 1247–1251. (b) Schalley, C. A. *Mass Spectrom. Rev.* **2001**, *20*, 253–309.

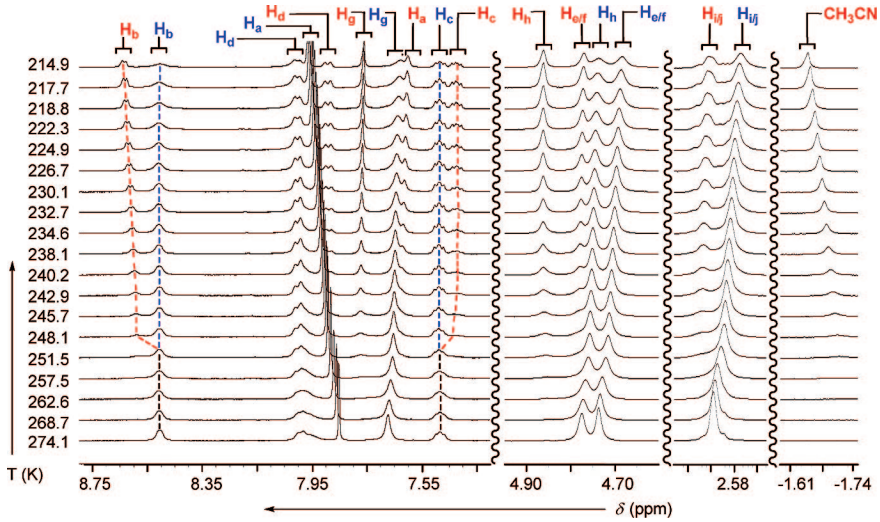

FIGURE 5. Variable temperature ^{1}H NMR spectra (400 MHz, $CD_3COCD_3/CDCl_3$= 5:3) of a solution of equimolar **1** and $[Cu(I)(CH_3CN)_4]PF_6$ (3.20 mM).

0.76 (stoichiometric balance) as independently fit parameters. The K_a value measured for the binding affinity is in excellent agreement with the one obtained in the ^{1}H NMR titration (Figure 2B). Interestingly, the assembly is strongly enthalpically driven, which is contrary to what was observed in folding of the same molecular basket with the Ag(I) cation ($\Delta H° = 3.0 \pm 0.1$ kcal/mol).[12b] The apparent gain in the enthalpy can, to a first approximation, be related to the substitution of labile acetonitrile ligands with pyridines in the assembly process. The apparent entropic balance ($\Delta S° = -0.25$ eu), though, was likely developed via combination of (a) differential solvation in the course of the complexation and (b) displacement of acetonitrile molecules in $[Cu(I)(CH_3CN)_4]PF_6$ with pyridines of **1**, operating by way of the chelate effect.[12,22] Respectively, our polydentate basket coordinates to Cu(I) with a much higher affinity ($\log \beta = 5.23$) than three monodentate pyridine ligands in acetonitrile ($\log \beta_3 = 3.26$).[22e,f]

Variable Temperature ^{1}H NMR Studies. Variable temperature ^{1}H NMR spectra of a solution ($CD_3COCD_3/CDCl_3 = 5:3$) of equimolar **1** and $[Cu(I)(CH_3CN)_4]PF_6$ (3.20 mM) revealed decoalescence of signals at 248.1 K (Figure 5). Two sets of peaks developed, with the ratio changing with external temperature. Each group of signals has been assigned to a C_3 symmetrical basket, $\mathbf{10_a}$ and $\mathbf{10_b}$ (Figure 6A), as reasoned below.

The appearance of an upfield singlet (−1.7 ppm, Figure 5) suggests that there is a guest residing inside the basket. Specifically, the inner space of **1** provides four benzene rings to surround an encapsulated compound, and thereby impose diamagnetic anisotropy on the protons situated in the shielding region.

Given its size, shape, and coordinating properties, acetonitrile can be envisioned to occupy the interior of this folded basket. In fact, solvent molecules are likely to compete for filling the inner space, but these solvent molecules are fully deuterated and therefore undetectable by ^{1}H NMR spectroscopy. A closer inspection of the two sets of ^{1}H NMR signals (Figure 5), revealed that the intensity of one set of signals does track with the upfield singlet. Namely, the integration of this set, assigned as $\mathbf{10_b}$, would consistently fit the upfield resonance to three protons, and therefore, is consistent with a CH_3 group in acetonitrile as the guest. Finally, when deuterated acetonitrile was used as the solvent, ^{1}H NMR measurements at low temperatures showed no upfield signal at −1.7 ppm, verifying the role of acetonitrile as the guest in $\mathbf{10_b}$.

2D COSY and ROESY ^{1}H NMR Studies. To fully assign the proton spin systems at low temperature (Figure 5), we conducted a series of 2D ^{1}H NMR experiments (190 K). Two-dimensional homonuclear (H, H) correlated (COSY) spectrum of a solution containing 2.60 mM **1** and 2.60 mM $[Cu(I)(CH_3CN)_4]PF_6$ ($CD_3COCD_3/CDCl_3 = 5:3$) revealed six distinct cross-peaks (Figure 6B). The peaks have been assigned to (a) $\mathbf{H_c}$ proton in $\mathbf{10_a}$ and $\mathbf{10_b}$, each coupled to the corresponding $\mathbf{H_b}$ and $\mathbf{H_d}$ protons contained by the pyridine flaps, and (b) two $\mathbf{H_{i/j}}$ protons, each coupled to its own bridgehead $\mathbf{H_h}$ proton (Figure 6A/B).

The characterization was further completed with ROESY experiments (Figure 6C), whereby the magnetization transfer through space was unsurprisingly observed for the juxtaposed $\mathbf{H_h}$ and $\mathbf{H_{i/j}}$ protons in both $\mathbf{10_a}$ and $\mathbf{10_b}$ and also for $\mathbf{H_h}$ and $\mathbf{H_g}$ in $\mathbf{10_b}$. More interestingly, a cross-peak corresponding to $\mathbf{H_{e/f}}$/$\mathbf{H_d}$ coupled nuclei was revealed in $\mathbf{10_b}$. Accordingly, the three protons must be arranged in space close enough to show the cross-correlation. The fact that the same cross peak was not observed in $\mathbf{10_a}$ suggests a distinctively different geometry for this stereoisomer, which could be of a more dynamic nature having no acetonitrile residing in its interior.

The observed chemical shifts for the protons in assemblies $\mathbf{10_a}$ and $\mathbf{10_b}$ (Figure 5B) provided additional information about the two structures in the equilibrium (Figure 6A). In particular, the $\mathbf{H_a}$ resonance in $\mathbf{10_b}$ exemplifies a considerable upper-field shift, $\Delta\delta = 0.40$ ppm, with respect to the same proton in $\mathbf{10_a}$. Presumably, C_3 symmetrical $\mathbf{10_b}$ incorporates three pyridine flaps more inclined to the basket base with each flap placing its $\mathbf{H_a}$ proton inside the cavity and against the shielding region of the encapsulated acetonitrile. With this geometry, the $\mathbf{H_d}$ proton must assume a position in between the "hinge" $\mathbf{H_{e/f}}$ protons whereby the magnetization transfer through space is facilitated (Figure 6C). In contrast, the downfield shifted $\mathbf{H_a}$ proton in $\mathbf{10_a}$

(22) (a) Zhang, B.; Breslow, R. *J. Am. Chem. Soc.* **1993**, *115*, 9353–9354. (b) Berger, M.; Schmidtchen, F. P. *Angew. Chem., Int. Ed.* **1998**, *37*, 2694–2696. (c) BaDjić, J. D.; Nelson, A.; Cantrill, S. J.; Turnbull, W. B.; Stoddart, J. F. *Acc. Chem. Res.* **2005**, *38*, 723–732. (d) Bea, I.; Gotsev, M. G.; Ivanov, P. M.; Jaime, C.; Kollman, P. A. *J. Org. Chem.* **2006**, *71*, 2056–2063. (e) Nilsson, K. B.; Persson, I. *Dalton Trans.* **2004**, 1312–1319. (f) Dachraoui, M. *Bull. Soc. Chim. Fr.* **1987**, *5*, 755–759.

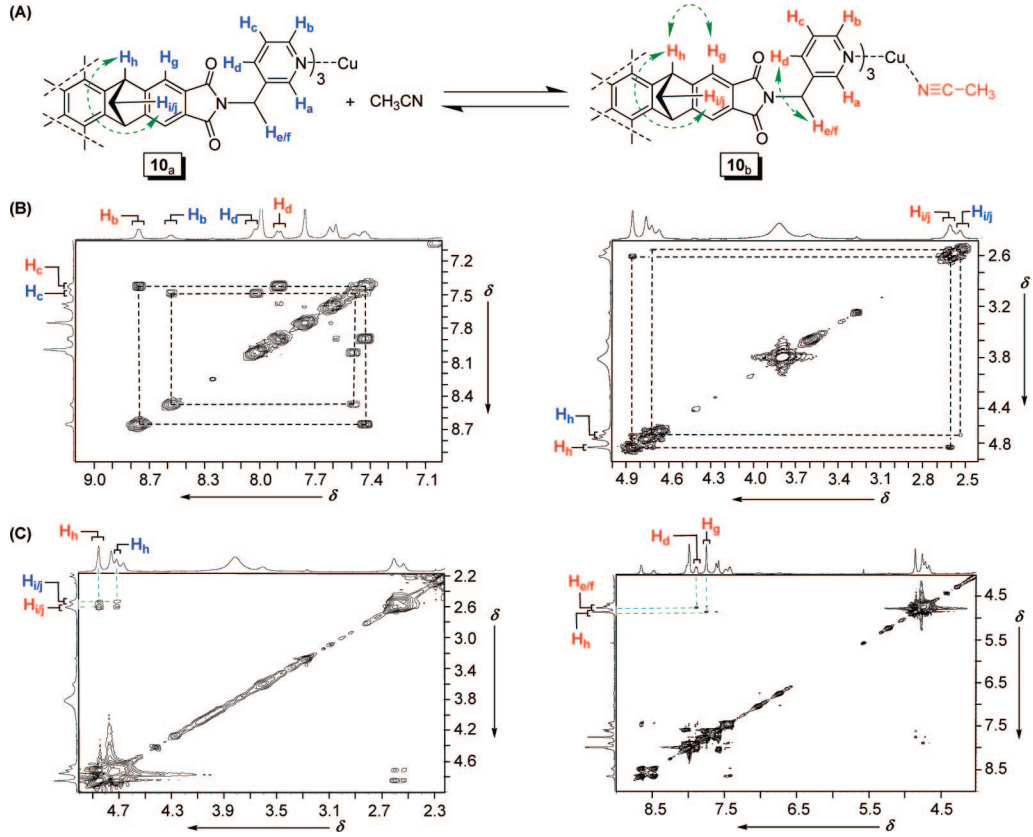

FIGURE 6. (A) ^{1}H NMR spectroscopic assignment of Cu(I)-folded molecular baskets $\mathbf{10_a}$ (blue) and $\mathbf{10_b}$ (red). (B) Selected regions of two-dimensional ^{1}H−^{1}H COSY spectrum (400 MHz, $CD_3COCD_3/CDCl_3$ = 5:3) of a solution of $\mathbf{10_{a/b}}$ (2.60 mM) at 190 K. (C) Selected regions of two-dimensional ^{1}H−^{1}H ROESY spectrum (400 MHz, $CDCl_3/CD_3COCD_3$ = 3:5, 100 ms mixing time) of a solution of $\mathbf{10_{a/b}}$ (2.60 mM) at 190 K.

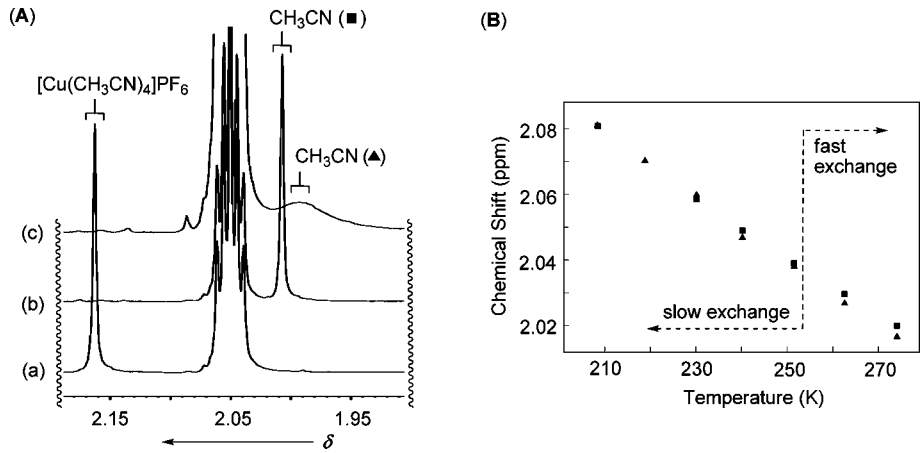

FIGURE 7. (A) Selected regions of ^{1}H NMR spectra (400 MHz, $CD_3COCD_3/CDCl_3$ = 5:3) of a solution of (a) $[Cu(I)(CH_3CN)_4]PF_6$ (3.20 mM), (b) CH_3CN (12.8 mM), and (c) $\mathbf{10_{a/b}}$ (3.20 mM) at 300 K. (B) ^{1}H NMR Chemical shifts for the methyl group in CH_3CN (400 MHz, $CD_3COCD_3/CDCl_3$ = 5:3) as a function of temperature: (■) a solution of acetonitrile (12.8 mM), and (▲) a solution of $\mathbf{10_{a/b}}$ (3.20 mM).

must be more remotely positioned with respect to the basket's interior, placing the corresponding $\mathbf{H_d}$ further away from the $\mathbf{H_{e/f}}$ protons, to minimize the magnetization transfer (Figure 6C). The structure of $\mathbf{10_a}$ is likely to resemble the earlier reported Ag(I)-folded molecular basket[12b] for which the ^{1}H NMR signals, and in particular $\mathbf{H_a}$, were observed at similar positions.

Apical Ligand(s). On the basis of the variable temperature and two-dimensional ^{1}H NMR experiments, it is evident that $\mathbf{10_b}$ features a tetracoordinate Cu(I) with a molecule of acetonitrile occupying its inner space (Figure 6A). Conversely, the ^{1}H NMR evidence was in favor of a solvent-filled $\mathbf{10_a}$ comprising a trigonal Cu(I) center coordinated to three pyridine flaps (Figure 7). That is to say, the transition metal lacks a molecule of acetonitrile as the labile fourth ligand, which in this situation would have been located on the outer side. The CH_3 protons of acetonitrile in $[Cu(I)(CH_3CN)_4]PF_6$ and completely metal-free acetonitrile resonate at 2.16 and 2.01 ppm (300 K), respectively (Figure 7A). ^{1}H NMR spectrum of $\mathbf{10_a/10_b}$ (300 K) revealed a broad methyl signal at 1.98 ppm (Figure 7A), indicating an intermediate interconversion rate between free and somewhat encapsulated acetonitrile.

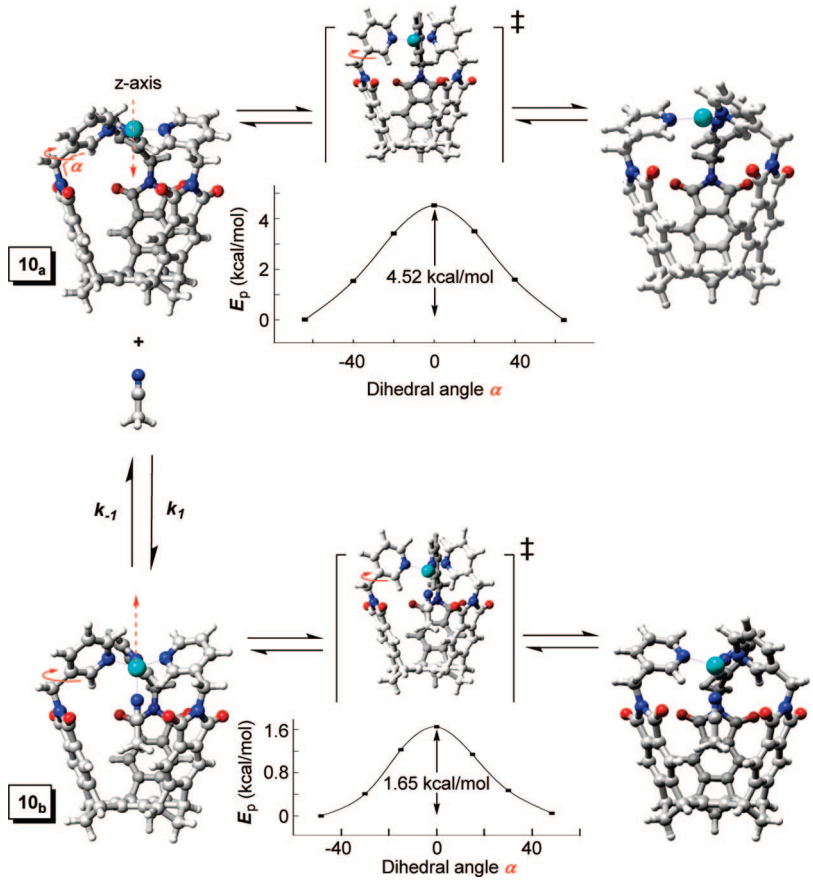

FIGURE 8. Energy minimized (DFT, BP86) conformations of $\mathbf{10_a}$ and $\mathbf{10_b}$. Synchronized rotation of the pyridine flaps about their N−C−C−C dihedral angle (α) was calculated to require 4.52 and 1.65 kcal/mol in $\mathbf{10_a}$ and $\mathbf{10_b}$, respectively.

In fact, when the signal contribution of the encapsulated acetonitrile was "taken away" (below 248 K; this molecule undergoes a slow in/out exchange on the ^{1}H NMR time scale), the remaining acetonitrile ^{1}H NMR signal became identical to that of the free acetonitrile (Figure 7B). The observation validates the equilibrium presented in Figure 6A, whereby the $\mathbf{10_{a/b}}$ conversion necessitates a molecule of acetonitrile to displace the solvent-filled (or empty) cavity in $\mathbf{10_a}$.[18] Indeed, the addition of neat acetonitrile to a solution of $\mathbf{10_{a/b}}$ shifted the equilibrium toward the greater formation of $\mathbf{10_b}$,[18] which is in accord with Le Chatelier's principle.

Density Functional Theory (DFT) Studies. The equilibrium between the two baskets $\mathbf{10_{a/b}}$ (Figure 6A) was further investigated computationally with DFT methods and the BP86 functional[23] in order to disclose the mechanistic details for the interconversion. Energy minimizations were initiated, each with a $\mathbf{10_a}$ or $\mathbf{10_b}$ starting geometry and a particular N−C−C−C torsional angle (α = 13−80°, Figure 8). It was found that the initial selection of the torsional angle would always give rise to one particular geometry (Figure 8).

The calculated results revealed that C_3 symmetric $\mathbf{10_b}$ (which contains acetonitrile as a guest) is more stable than the empty $\mathbf{10_a}$ and an isolated acetonitrile by −11.0 kcal/mol (Δ*E*). Both $\mathbf{10_a}$ and $\mathbf{10_b}$ are helically twisted, and the empty or full basket can be arranged in an *M* or *P* orientation for the gearing of the aromatic units. The pyridine flaps in $\mathbf{10_b}$ are tilted relative to the base (α = 48.2°) and with the nitrogen atoms coordinated to Cu(I). Furthermore, the Cu(I) also holds a molecule of acetonitrile toward the base of the basket, thereby pointing the hydrogens of the acetonitrile toward the basket's aromatic walls. In comparison, the trigonal (and empty) assembly $\mathbf{10_a}$ was computed to also contain pyridine moieties arranged in the helical fashion, yet more tilted to the base (α = 64.2°, Figure 8). Evidently, the presence of the internal acetonitrile guest in $\mathbf{10_b}$ demands a relocation of the Cu(I) cation down into the cavity of the basket, along the assembly's *z* axis, which is synchronized with a gradual twist of the pyridine gates (Δα = 16°). The calculated thermodynamic bias of −11 kcal/mol is in favor of the formation of $\mathbf{10_b}$, relative to an empty basket $\mathbf{10_a}$.

Furthermore, one can envision that the acetonitrile guest replaces a coordinated solvent (e.g., acetone) molecule on the outside of the basket,[18] and in that case, the calculated thermodynamic (Δ*E*) bias is −3.5 kcal/mol, once again in favor of acetonitrile being inside the cavity ($\mathbf{10_b}$). This latter value is in good accord with experiment (Δ*H*° = −3.3 kcal/mol, see below). Interestingly, the synchronized rotation of the pyridine flaps about their axis, in $\mathbf{10_a}$ and $\mathbf{10_b}$, allows for each of the assemblies to flutter between two enantiomeric, right-handed *P* and left-handed *M*, helical forms (Figure 8). The interconversion comes with a small energetic penalty of 4.52 and 1.65 kcal/mol for $\mathbf{10_a}$ and $\mathbf{10_b}$, respectively (BP86, Figure 8). The calculated activation barriers are thus in line with the observed appearance of only one signal for the diastereotopic $\mathbf{H_{e/f}}$ protons in variable temperature ^{1}H NMR experiments (Figure 5).

(23) (a) Perdew, J. P. *Phys. Rev. B* **1986**, *33*, 8822. (b) Becke, A. D. *Phys. Rev. A* **1998**, *38*, 3098–4100.

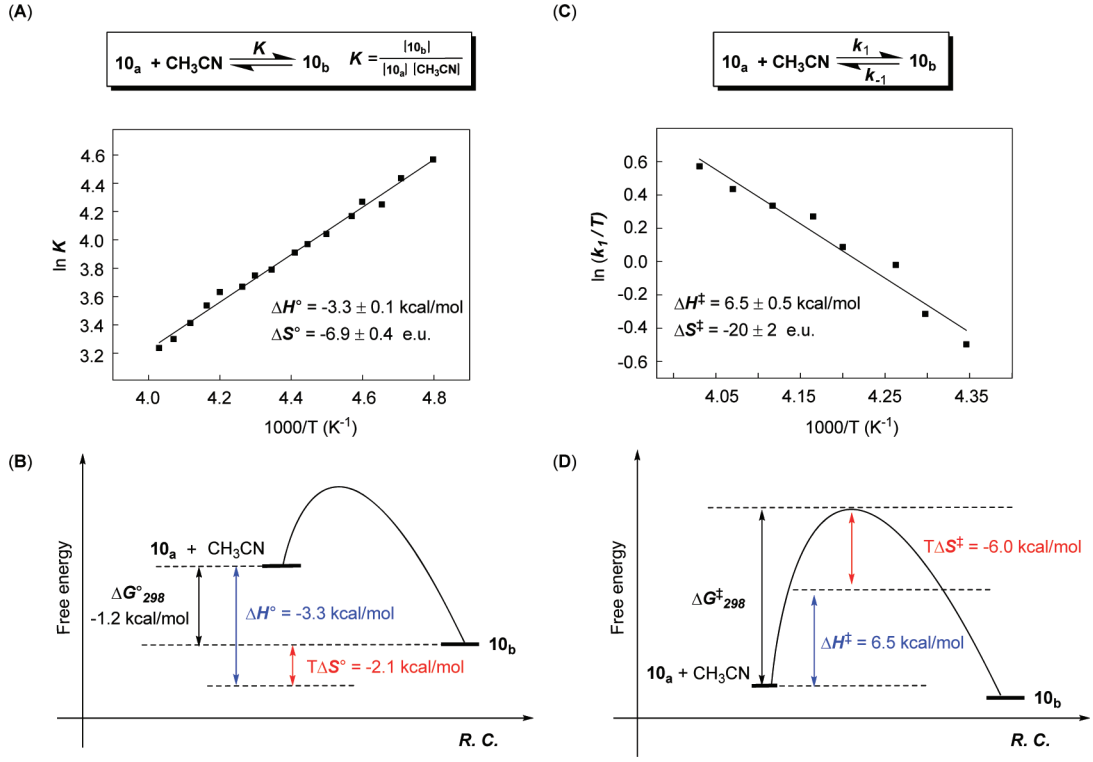

FIGURE 9. (A) Van't Hoff plot and (B) the thermodynamic parameters for the $\mathbf{10_{a/b}}$ interconversion. (C) Eyring plot and (D) the activation parameters for the $\mathbf{10_{a/b}}$ interconversion.

Thermodynamics and Kinetics of the Exchange. With solid experimental evidence for the interconversion of folded molecular baskets $\mathbf{10_a}$ and $\mathbf{10_b}$, we further examined the system's dynamics and thermodynamics. From variable temperature ^{1}H NMR experiments (Figure 5), integration of the signals at each temperature afforded equilibrium association constants (K_a). Once the data were integrated in a van't Hoff plot, the thermodynamic parameters for the conversion of $\mathbf{10_a}$ into $\mathbf{10_b}$ became available (Figure 9A and B).

In essence, the incorporation of an acetonitrile molecule inside the basket is strongly driven by enthalpy ($\Delta H° = -3.3 \pm 0.1$ kcal/mol). Such apparent gain in enthalpy can, for the most part, be viewed as a result of the formation of an additional metal-to-ligand coordination bond taking place in the encapsulation event. The weak noncovalent forces, the basket's strain, and solvation effects all contribute to the net exothermicity, but presumably to a smaller degree. The observed loss in entropy ($\Delta S° = -9.4 \pm 0.4$ eu, Figure 9A and C), is congruent with the complete immobilization of a molecule of acetonitrile and the release of a "loosely" encapsulated solvent molecule during the formation of $\mathbf{10_b}$.

The interconversion of $\mathbf{10_a/10_b}$, in addition, gave rise to the exchange of NMR resonances of proton nuclei experiencing different chemical environments. Hence, we used a total band-shape analysis to obtain the apparent rate constants k_1/k_{-1} (Figure 10)[24] and, from an Eyring plot, the activation parameters for the dynamic $\mathbf{10_a/10_b}$ equilibrium (Figure 9C and D). The resonance for $\mathbf{H_b}$ in $\mathbf{10_a/10_b}$ was observed as one signal at high temperatures (Figure 10). At lower temperatures, however, this

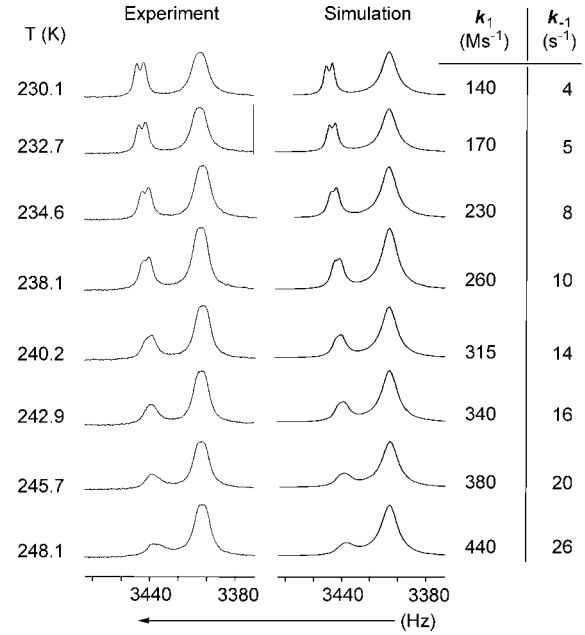

FIGURE 10. Experimental and simulated (Maple 11) signals for the $\mathbf{H_b}$ protons in $\mathbf{10_b}$ and $\mathbf{10_a}$, respectively. Apparent second- and first-order (k_1 and k_{-1}) rate constants for the $\mathbf{10_{a/b}}$ interconversion at different temperatures.

resonance decoalesced into two signals whose intensity ratio and line shape were a function of temperature; the downfield signal was observed as a doublet, while the upfield signal was a broad peak, presumably a doublet. Thus, two unequally populated and coupled spin states, originating from the $\mathbf{H_b}$ nucleus, were generated from the same nucleus residing in two magnetically different environments, provided by $\mathbf{10_a}$ and $\mathbf{10_b}$. To develop an appropriate kinetic density matrix[18] and solve

(24) (a) Kaplan, J. J.; Fraenkel, G. In *NMR of Chemically Exchanging Systems*; Academic Press: New York, 1980. (b) Pons, M.; Millet, O. *Prog. Nucl. Magn. Reson. Spectrosc.* **2001**, *38*, 267–324. (c) Bain, A. D.; Rex, D. M.; Smith, R. N. *Magn. Reson. Chem.* **2001**, *39*, 122–126. (d) Bain, A. D. *Prog. Nucl. Magn. Reson. Spectrosc.* **2003**, *43*, 63–103.

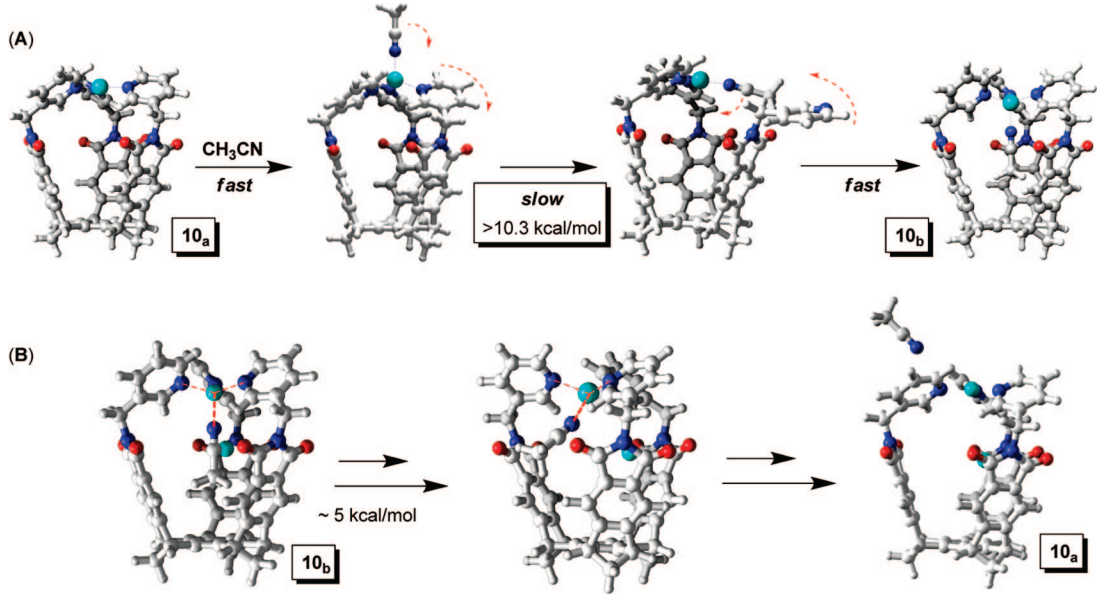

FIGURE 11. Gated- (A) and slippage-based (B) mechanisms for the $\mathbf{10_{a/b}}$ interconversion have been proposed, and further assessed by DFT (BP86) calculations.

for the equilibrium kinetics, a dissociative mechanism was hypothesized to operate in acetonitrile departing from the basket interior. The effective chemical exchange rate constants, which are directly relevant to the NMR experiments, were given as: $k_f = k_1 \cdot$[acetonitrile] and $k_b = k_{-1}$. From the temperature dependence of the $\mathbf{H_b}$ resonance's line shape (Figure 10), the fitting procedure gave the apparent rate constants (k_1 and k_{-1}) for the equilibrium at different temperatures. From the Eyring plot (Figure 9B), the activation enthalpy for incorporating acetonitrile into $\mathbf{10_a}$ was found to be positive ($\Delta H^{\ddagger} = 6.5 \pm 0.5$ kcal/mol), while the activation entropy was negative ($\Delta S^{\ddagger} = -20 \pm 2$ eu). Evidently, the transition state for the encapsulation is more ordered with respect to the ground state ($\Delta S^{\ddagger} < 0$), which is in agreement with a mechanism whereby a molecule of acetonitrile combines with an "empty" basket in the reaction's rate-determining step (Figure 8).

Encapsulation Mechanism. What is the guest exchange mechanism for these Cu(I)-folded molecular baskets? One can envision a scenario (Figure 11A) for which the empty basket $\mathbf{10_a}$ binds a molecule of acetonitrile on its outer side. Subsequently, a pyridine flap dissociates from the transition metal to facilitate the coordinated acetonitrile to turn inside the basket. Although feasible, both experiment and theory are less in favor of such a mechanistic pathway. First, the experimental evidence for the outer coordination of acetonitrile is lacking. Second, the thermodynamic energy difference for cleaving a pyridine unit coordinated to Cu(I) and internalization of the CH_3CN guest requires at least 10.3 kcal/mol.

On the contrary, the experimental activation energy ($\Delta H^{\ddagger}$) is 6.5 kcal/mol for the conversion of $\mathbf{10_a}$ into $\mathbf{10_b}$. Furthermore, gas-phase collision-induced dissociation experiments by Rodgers and co-workers has revealed that the bond dissociation energy ($\Delta H°$, 0K) for the removal of a pyridine unit from the $Cu^+(pyridine)_3$ complex to be on the order of 20 kcal/mol.[25] Our DFT calculations suggested that over 10.3 kcal/mol (ΔE) is required for such a rate-determining step to take place (Figure 11A).

A more feasible mechanism (Figure 11B), however, encloses an in/out exchange of acetonitrile through the aperture in $\mathbf{10_{a/b}}$ that, in fact, requires for the basket to expand slightly for the guest to enter or to leave the cavity. To evaluate the elasticity of the host,[26] we examined (BP86) the passage of acetonitrile from the center of the cavity and along a reaction trajectory defined by the (basket-center)···$\underline{C}H_3CN$ or (basket-center)···$CH_3C\underline{N}$ distance.[18] The guest escape (entrance) through the host "skin" was revealed to be rather facile; it takes roughly 5 kcal/mol to drive the methyl group through the host aperture, without a considerable coordination-bond rupture to Cu(I), Figure 11B. In view of that, we deduce that the second mechanism is more likely to be operating for the guest exchange. Importantly, by varying the host structure, as well as the guest's electronic properties, size and shape, the notion of manipulating the exchange pathway to direct molecular transport in artificial environments is becoming more feasible.

Conclusions

Transition-metal-mediated folding of molecular baskets proves to be a practical strategy for creating dynamic inner space suitable for studying molecular transport in synthetic systems. Diamagnetic and soft Cu(I) has, in this work, been demonstrated to effectively chelate the pyridine "flaps", positioned at the rim of the basket, and fold them in a helical fashion. The coordination led to a complete constriction of a chiral and dynamic space inside the molecular container. The transition metal was revealed to coordinate to a molecule of acetonitrile in the cavity of the basket. This, in turn, restricted the mobility of the guest, which points its methyl group against the aromatic walls of the host, and was clearly discernible by ^{1}H NMR spectroscopy. Importantly, the immobilized guest was in equilibrium with "free" acetonitrile in bulk solution in an exchange process occurring via a slight expansion of the host aperture; a gated transport mediated by opening and closing of the

(25) (a) Vitale, G.; Valina, A. B.; Huang, H.; Amunugama, R.; Rodgers, M. T. *J. Phys. Chem. A* **2001**, *105*, 11351–11364. (b) Rannulu, N. S.; Rodgers, M. T. *J. Phys. Chem. A* **2007**, *111*, 3465–3479.

(26) (a) Sheu, C.; Houk, K. N. *J. Am. Chem. Soc.* **1996**, *118*, 8056–8070. (b) Houk, K. N.; Nakamura, K.; Sheu, C.; Keating, A. E. *Science* **1996**, *273*, 627–629. (c) Wang, X.; Houk, K. N. *Org. Lett.* **1999**, *1*, 591–594. (d) Fyfe, M. C. T.; Raymo, F. M.; Stoddart, J. F. In *Stimulating Concepts in Chemistry*; Wiley-VCH: Weinheim, 2000; pp 211−220. (e) Davis, A. V.; Raymond, K. N. *J. Am. Chem. Soc.* **2005**, *127*, 7912–7919.

"flaps" was presented as a less likely mechanistic scenario. It is the manipulation of the guest's encapsulation via metal-to ligand coordination that holds a promise for directing chemical reactivity in dynamic and confined media.

Experimental Section

Compound 6. A carbon tetrachloride (150 mL) solution of **5** (5.37 g, 27.2 mmol) and freshly distilled dimethyl acetylenedicarboxylate (5.32 g, 37.4 mmol) was allowed to stir at reflux for 12 h. The solvent was removed at a reduced pressure to yield an amber oil (9.24 g). The oil was dissolved in dichloromethane (200 mL) and solid 2,3-dichloro-5,6-dicyano-*p*-benzoquinone (7.10 g, 31.3 mmol) was added. The mixture was mechanically stirred under argon (12 h, rt), before it was "washed" with a saturated aqueous $NaHCO_3$ solution (3 × 200 mL) and dried ($MgSO_4$), and the organic layer was concentrated in vacuo. The solid residue was purified by column chromatography (SiO_2, CH_2Cl_2) to yield **6** (6.54 g, 71%) as a colorless oil. ^{1}H NMR (400 MHz, $CDCl_3$, 298 K): δ 2.35 (1H, d, J = 7.6 Hz), 2.63 (^{1}H, d, J = 8.0 Hz), 3.85 (1H, s), 3.88 (6H, s), 4.00 (1H, s), 6.73 (1H, d, J = 3.2 Hz), 7.51 (1H, s), and 7.65 ppm (1H, s); ^{13}C NMR (100 MHz, $CDCl_3$, 298 K): δ 51.7, 52.6, 52.7, 58.2, 68.8, 121.5, 122.1, 128.9, 130.1, 135.8, 139.8, 153.3, 153.9, 168.1, and 168.4 ppm; HRMS (EI): *m*/*z* calcd for $C_{15}H_{14}BrO_4$ 337.0075 $[M + H]^+$; found 337.0061.

Compound 7. To a solution of dry diisopropylamine (830 μL, 5.90 mmol) in THF (20 mL) at −78 °C was added *n*-butyl lithium (1.6 M in hexanes, 3.60 mL, 5.76 mmol), and the mixture was stirred for 40 min under an atmosphere of argon. A solution of **6** (1.50 g, 4.45 mmol) in THF (10 mL) was then added dropwise over a period of 10 min, and the resulting mixture was stirred for an additional 30 min. Following, a solution of trimethyltin chloride (937 mg, 4.76 mmol) in THF (10 mL) was added dropwise over a period of 10 min, and the resulting mixture was gradually warmed to room temperature over a period of 3 h. Aqueous NH_4Cl (4 mL) was used to quench the base, followed with the removal of the organic layer in vacuo. The solid residue was washed with water (60 mL) and extracted with diethyl ether (2 × 70 mL). The combined organic phase was dried ($MgSO_4$) and concentrated in vacuo. The solid residue was purified by column chromatography (SiO_2, hexanes/ethyl acetate, 2:1) to yield **7** as a white solid (1.59 g, 72%). Mp 139−140 °C; ^{1}H NMR (400 MHz, CDCl3, 27 °C): δ 0.24 (9H, t, J = 40 Hz), 2.27 (1H, d, J = 7.6 Hz), 2.57 (1H, d, J = 7.6 Hz), 3.91 (7H, s), 4.09 (1H, s), 7.47 (1H, s), and 7.65 ppm (1H, s); ^{13}C NMR (100 MHz, $CDCl_3$, 27 °C): δ −9.3, 52.5, 52.6, 57.0, 60.2, 68.4, 121.1, 122.0, 129.0, 129.8, 147.0, 152.2, 153.6, 154.0, 168.4, and 168.5 ppm; HRMS (EI): *m*/*z* calcd for $C_{16}H_{16}BrO_4Sn$ 500.9723 $[M + H]^+$; found 500.9687.

Compound 4_{syn}.[12a] A mixture of **7** (1.09 g, 2.18 mmol) and $Cu(NO_3)_2 \cdot 2.5H_2O$ (2.53 g, 10.9 mmol) in acetone (53 mL) was stirred at 50 °C overnight. The solvent was removed in vacuo and the remaining residue was washed with a 10% aqueous NH_3 solution (60 mL) and extracted with diethyl ether (3 × 100 mL). The combined phase was dried ($MgSO_4$) and concentrated in vacuo. The solid residue was purified by column chromatography (SiO_2, dichloromethane/acetone, 9:1) to yield $\mathbf{4}_{syn}$ (75.8 mg, 13.6%) as a white solid. Mp 215 °C; ^{1}H NMR (400 MHz, $CDCl_3$, 27 °C): δ 2.54 (6H, s), 3.80 (18H, S), 4.43 (6H, s), and 7.45 ppm (6H, s); ^{13}C NMR (100 MHz, $CDCl_3$, 27 °C): δ 48.8, 52.3, 65.4, 121.6, 129.8, 137.8, 152.8, and 168.1 ppm. HRMS (ESI): *m*/z calcd for $C_{45}H_{36}O_{12}Na$ 791.2099 $[M + Na]^+$; found 791.2098.

Dynamic ^{1}H NMR Studies. Compounds $\mathbf{10_a}$ and $\mathbf{10_b}$ showed a proton resonance H_b at 8.50 and 8.63 ppm, respectively. The resonances consisted of a 1:1 doublet due to scalar coupling to a single neighboring proton H_c, J = 4.6 Hz. With increasing temperature, above 230.1 K, the two doublets progressively average to a single doublet (Figure 5). This is clearly the result of a fast equilibrium exchange process whose rate lies on the NMR time scale. We assumed that the spin state of the proton neighbor does not change during the exchange process.

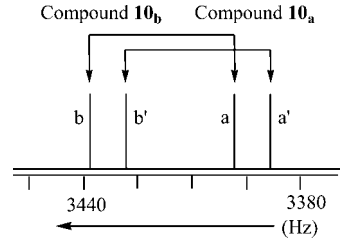

Thus, we simulated the system as consisting of two separately averaging unequal doublets as indicated in the given diagram. Each peak was treated as being due to a pseudo half-spin transition. The four transitions are labeled from left to right as b, b′ ($\mathbf{10_b}$) and a, a′ ($\mathbf{10_a}$), with frequencies ω_b, $\omega_{b'}$, ω_a, $\omega_{a'}$ (radians·s^{-1}) and intrinsic line width $1/T$ (s^{-1}). The pseudo-first-order rate constants are $k^1_{b\rightarrow a}$, $k^1_{b'\rightarrow a'}$, $k^1_{a\rightarrow b}$, and $k^1_{a'\rightarrow b'}$. Note that the first pair is identical, as is the last pair. Required elements of the density matrix are ρ_b, $\rho_{b'}$, ρ_a, and $\rho_{a'}$. The four first-order coupled inhomogeneous density matrix equations used in the fitting of the experimental spectra are displayed (eq 1).

$$\begin{bmatrix} i(\omega-\omega_b)-(1/T)-k^1_{b\rightarrow a} & k^1_{b\rightarrow a} & 0 & 0 \\ k^1_{a\rightarrow b} & i(\omega-\omega_a)-(1/T)-k^1_{a\rightarrow b} & 0 & 0 \\ 0 & 0 & i(\omega-\omega_{b'})-(1/T)-k^1_{b'\rightarrow a'} & k^1_{b'\rightarrow a'} \\ 0 & 0 & k^1_{a'\rightarrow b'} & i(\omega-\omega_{a'})-(1/T)-k^1_{a'\rightarrow b'} \end{bmatrix} \begin{bmatrix} \rho_b \\ \rho_{b'} \\ \rho_a \\ \rho_{a'} \end{bmatrix} = i \begin{bmatrix} 1 \\ 1 \\ 1 \\ 1 \end{bmatrix}$$

Equation 1 is solved for the four elements of the density matrix as a function of frequency. The absorption is obtained from the imaginary part of the appropriated weighted sum of the latter ρ values (eq 2), where the (a), (a′), (b), and (b′) are concentrations. Note that (a) = (a′), (b) = (b′), $k^1_{b\rightarrow a} = k^1_{b'\rightarrow a'}$, and $k^1_{a\rightarrow b} = k^1_{a'\rightarrow b'}$ and all that is needed for the concentration terms is the ratio (a)/(b). Comparison of the observed and calculated line shapes provided the pseudo-first-order rate constants. Their relationship with the proposed interconversion (Figure 6A) was resolved with the assistance of the eqs 3−6.

$$\mathrm{Abs} = -\mathrm{Im}[(a)\rho a + (a')\rho a' + (b)\rho b + (b')\rho b'] \quad (2)$$

$$k'_{a\rightarrow b} = k_f(CH_3CN) \quad (3)$$

$$k'_{b\rightarrow a} = k_r \quad (4)$$

$$k_f/k_r = (b)/[(a)(CH_3CN)] = K \quad (5)$$

$$k'_{a\rightarrow b}/k'_{b\rightarrow a} = K(CH_3CN) \quad (6)$$

Acknowledgment. This work was financially supported with funds obtained from the Ohio State University, and the National Science Foundation under CHE-0716355. Generous computational resources were provided by the Ohio Supercomputer Center.

Supporting Information Available: Additional experimental, computational methods and results, and spectra for all new compounds. This material is available free of charge via the Internet at http://pubs.acs.org.

JO800748K